Impact and extinction in remarkably complete Cretaceous-Tertiary boundary sections from Demerara Rise, tropical western North Atlantic

Kenneth G. MacLeod[†]
Department of Geological Sciences, University of Missouri, Columbia, Missouri 65211, USA

Donna L. Whitney[‡]
Department of Geology and Geophysics, University of Minnesota, Minneapolis, Minnesota 55455, USA

Brian T. Huber[§]
Department of Paleobiology, Smithsonian National Museum of Natural History, Washington, DC 20013-7012, USA

Christian Koeberl[#]
Department of Geological Sciences, University of Vienna, Althanstrasse 14, A-1090 Vienna, Austria

ABSTRACT

Ocean Drilling Program (ODP) Leg 207, on the Demerara Rise in the western tropical North Atlantic, recovered multiple Cretaceous-Paleogene boundary sections containing an ejecta layer. Sedimentological, geochemical, and paleontological changes across the boundary closely match patterns expected for a mass extinction caused by a single impact. A normally graded, ~2-cm-thick bed of spherules that is interpreted as a primary air-fall deposit of impact ejecta occurs between sediments of the highest Cretaceous *Plummerita hantkeninoides* foraminiferal zone and the lowest Paleogene P0 foraminiferal zone. There are no other spherule layers in the section. In addition to extinction of Cretaceous taxa, foraminiferal abundance drops from abundant to rare across the boundary. Ir concentrations reach a maximum of ~1.5 ppb at the top of the spherule bed, and the Ir anomaly is associated with enrichment in other siderophile elements. We attribute the unusually well-preserved and relatively simple stratigraphy to the fact that Demerara Rise was close enough (~4500 km) to the Chicxulub impact site to receive ~2 cm of ejecta, yet was far enough away (and perhaps sheltered by the curve of northern South America) to have been relatively unaffected by impact-induced waves.

[†]E-mail: macleodk@missouri.edu.
[‡]E-mail: dwhitney@umn.edu.
[§]E-mail: huberb@si.edu.
[#]E-mail: christian.koeberl@univie.ac.at.

Keywords: Cretaceous-Paleogene boundary, mass extinction, impact, Demerara Rise, Ir anomaly, ODP Site 1259, ODP Leg 207.

INTRODUCTION

Discussion of the cause of the Cretaceous-Paleogene (commonly, Cretaceous-Tertiary or K-T) boundary event has evolved considerably in the two and a half decades since the asteroid impact hypothesis first gained prominence (e.g., Alvarez et al., 1980; Smit and Hertogen, 1980). That a major impact with widespread consequences occurred at or near the time of the K-T boundary is now generally accepted (e.g., papers in Koeberl and MacLeod, 2002), but a few workers dispute whether a single impact at Chicxulub alone adequately explains global paleontological and sedimentological patterns across the boundary (e.g., Adatte et al., 2002; Keller et al., 2004; Stüben et al., 2005). Most well-studied marine K-T sections are either relatively proximal (within 2500 km) to Chicxulub or relatively distal (more than 7000 km) from Chicxulub, with intermediate distances represented dominantly by terrestrial sites (e.g., Smit, 1999; Claeys et al., 2002). Interpretation of the few described intermediate marine K-T sites is complicated by the presence of redeposited material (e.g., Olsson et al., 1997; Smit, 1999), and arguments and counterarguments regarding the interpretation of marine K-T records have not been resolved.

Briefly summarized, disagreements for relatively proximal sites (Gulf of Mexico and nearby regions) center on how many impacts occurred and on their timing relative to K-T extinctions. Papers favoring a single impact emphasize the extreme nature of a Chicxulub-scale impact compared to background processes (e.g., Bourgeois et al., 1988; Olsson et al., 1996; Smit et al., 1996; Bralower et al., 1998; Klaus et al., 2000; Arz et al., 2004; Smit et al., 2004; Alegret et al., 2005; Schulte et al., 2006). These studies propose that the Chicxulub impact initiated multiple, temporally overlapping sedimentological processes, including vaporization-condensation of impactor and target material; ballistic distribution of ejecta; settling of ejecta through a water column; suspension/redeposition, winnowing, and traction transport of previously deposited material under the influence of tsunami and seiches; and gravity flows induced by seismic activity. Together these processes could have resulted in the deposition of a complex sequence of potentially quite thick and spatially variable basal Paleocene strata that accumulated within a few hours to few years of the impact.

Alternative hypotheses for the genesis of anomalous deposits in the vicinity of the K-T boundary emphasize lithologic variability and include bed-by-bed interpretations of the stratigraphic record at each site (e.g., Keller et al., 1988, 2004; Stinnesbeck et al., 2002). In other words, individual beds are generally considered to be distinct, largely independent, sedimentological events. Explicitly or implicitly, these interpretations invoke background rates and processes in estimating time represented by each bed and conclude that multiple impacts, other ecological stresses, and gradual and/or stepwise extinction patterns are critical features of the K-T boundary interval. Regardless of one's opinions of the accuracy of sedimentological and paleontological arguments (e.g., compare Arz et al., 2004; Keller et al., 2004; Smit et al., 2004),

GSA Bulletin; January/February 2007; v. 119; no. 1/2; p. 101–115; doi: 10.1130/B25955.1; 9 figures; 2 tables.

proximal deposits are undeniably complex and are laterally variable.

Controversy at distal K-T sites has focused on stratigraphic completeness and the ecological implications of observed last occurrences of foraminifera and nannoplankton. Evidence for impact and other boundary signatures at distal sites is generally concentrated in a few millimeters to centimeters of section across which there are major changes in fossil assemblages (e.g., Smit, 1999). However, these sections commonly contain Cretaceous taxa with last occurrences above or below the evidence for impact, and key zonal indicators may not be observed. Under the impact hypothesis, the stratigraphic coincidence of indicators of impact and paleontological change is attributed to virtual coincidence in time of these events preserved in depositional settings that largely lack the extreme depositional processes and sedimentation rates of proximal sites. The presence of Cretaceous taxa above the boundary is explained as the product of reworking (e.g., Pospichal, 1996; MacLeod et al., 2001; Huber et al., 2002; Bown, 2005), and last occurrences of taxa below the boundary as sampling artifacts (e.g., Signor and Lipps, 1982; Ginsburg, 1997). The absence of zonal markers is attributed to the sites being outside the biogeographic or facies preferences of the index taxa, failure to resolve geologically short intervals of time due to low sedimentation rates resulting in deposits that are thin relative to the scale of bioturbation, or drilling disturbance (e.g., Norris et al., 1999; MacLeod et al., 2001; Huber et al., 2002).

Papers favoring multiple stresses and/or a gradual K-T transition have argued that the relative sharpness of the boundary at distal sites is an artifact of incomplete records as indicated, for example, by the absence of the earliest Danian P0 zone and latest Maastrichtian index fossil *Plummerita hantkeninoides* in deep-sea sites. Further, last occurrences below and above the boundary have been interpreted as pre-impact extinctions and postimpact survivorship, respectively (e.g., MacLeod and Keller, 1991; Ginsburg, 1997; MacLeod et al., 1997). As with arguments for proximal sites, because the dispute resides more in interpretation than in observation, it is difficult to resolve with existing samples.

This paper describes new samples from the K-T boundary interval on Demerara Rise recovered during Ocean Drilling Program (ODP) Leg 207. Demerara Rise is a submarine plateau that extends from the NE coast of South America (Fig. 1) and was one of the last points of contact between Africa and South America as the Atlantic Ocean basins opened. The Demerara sections contain diverse foraminiferal assemblages and well-expressed sedimentological and geochemical variations with minimal drilling disturbance or stratigraphic complexities. That is, these samples provide access to exactly the type of new observations that can be used to address many of the ambiguities just outlined.

MATERIALS AND METHODS

At 65.5 Ma, Demerara Rise was ~4500 km SE of Chicxulub (Fig. 1). During ODP Leg 207, 13 holes at 5 sites were drilled on the northern slope of Demerara Rise where shallowly buried, horizontally bedded Upper Cretaceous–Paleogene sediments overlie Aptian and older, faulted, siltstones and claystones deposited during the rifting of South America and Africa. The postrifting sequence starts with a Cenomanian–lower Campanian interval composed of 50–90 m of finely laminated, organic-rich clayey siltstones with variable carbonate content ("black shales" sensu Schlanger and Jenkyns, 1976). The upper portion of the black-shale interval is condensed and grades into an overlying interval, up to several hundred meters thick, of upper Campanian–Eocene pelagic and hemipelagic chalks, clayey chalks, and claystones deposited at bathyal paleodepths. In 6 of the 13 holes drilled, the K-T boundary was recovered and is marked by a spherule-bearing horizon. Drilling disturbance compromised two of these records, but a well-preserved spherule bed and adjacent strata were recovered in Holes 1258A, 1259B, 1259C, and 1260A (Erbacher et al., 2004).

This study focuses on material from Holes 1259B and 1259C. The spherule layer is in interval 13R-1, 47–49 cm in Hole 1259B (Fig. 2) and 8R-5, 98–100 cm in Hole 1259C. A suite of 34, 5–10 cm^3 bulk samples was collected from core 8R in Hole 1259C. Seven samples are from the ~3.5 m of core below the spherule bed and the rest are from the ~6 m of core above that horizon. In addition, 2 samples (~1 cm^3) were collected from the spherule layer—the lower sample spanned the lower centimeter of spherule layer as well as the underlying lower white layer, the upper sample spanned the upper centimeter of the spherule layer. From Hole 1259B, 8 ~0.5 cm^3 samples with 0.25 cm spacing were collected from the 2 cm immediately above the spherule layer, and the lowest of these 8 samples was from the upper white zone (Fig. 2). Portions of the bulk samples were disaggregated using kerosene and washed on a 63 μm screen (Cretaceous and younger Danian samples) or 38 μm screen (basal Danian samples). The resulting coarse residues were used to document the distribution of planktic foraminifera.

For the coincidence spectrometry method (to analyze Ir contents), the rock samples were crushed manually in a plastic wrap, mechanically in an alumina jaw crusher, and then powdered using automatic agate mills. About 100 mg of the material was sealed in quartz vials of 4 mm outer diameter. The samples and standards were packed and irradiated for 48 h at the TRIGA MARK II reactor of the Institute of Isotopes, Budapest, Hungary, at a flux of ~7.1013 n cm^{-2} s^{-1}. After a cooling period of three months, the samples were gamma-counted for about one day each.

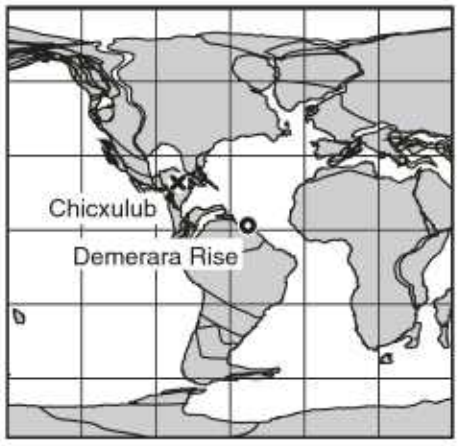

Figure 1. Position of Demerara Rise (O) and the Chicxulub impact site (X) on a paleogeographic reconstruction of the end of the Cretaceous (map from the Ocean Drilling Stratigraphic Network, www.odsn.de).

Geological reference materials were used as standards. An aliquot of powdered Allende standard meteorite from the Smithsonian Institution (a carbonaceous chondrite, type CV3) containing 740 ppb Ir was mixed intimately with high-purity quartz powder (Merck) and homogenized in a boron carbide mortar. To avoid errors due to the inhomogeneity of the Allende meteorite, dilution series of four standards were prepared directly in high-purity quartz vials ("Suprapur"), with contents between 48 and 325 ppt Ir. For the standard dilution series, a regression analysis was done to get the interpolated values of their volumes. Some of our measurements was close to the detection limit for the current irradiation and measurement parameters, which were between 5 and 30 ppt, depending on the rock type analyzed. Precision of the analyses were usually on the order of 5–15 rel%. Further details of the procedure, as well as on the instrumentation, are given in Koeberl and Huber (2000).

For petrographic studies and for X-ray mapping of major- and minor-element abundances, four thin sections were prepared from a continuous, 22-cm-long slab (Hole 1259B, 13R-1, 36–58 cm), which spans the upper 9 cm of the

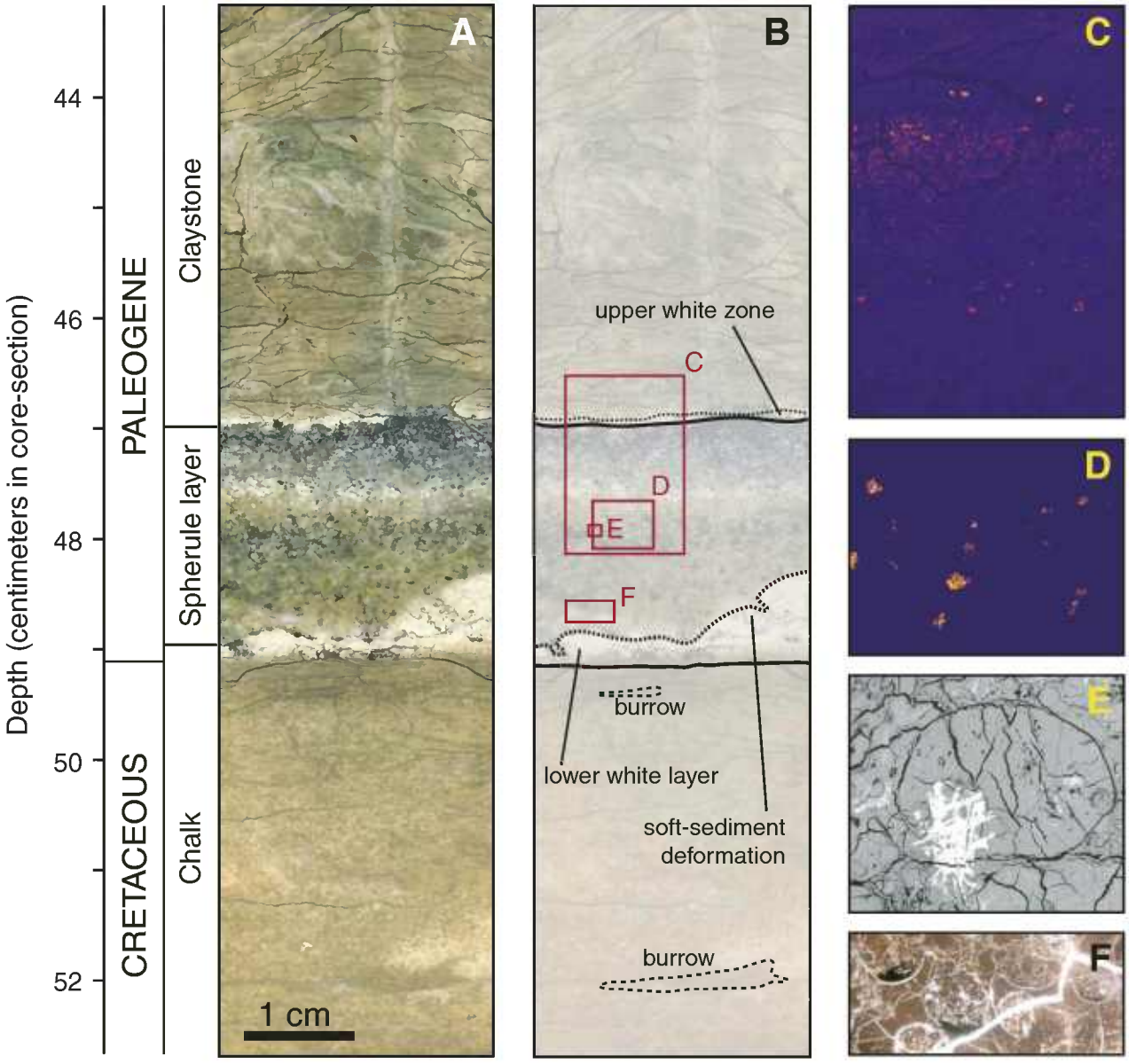

Figure 2. The Cretaceous-Tertiary (K-T) boundary in Ocean Drilling Program (ODP) Hole 1259B. (A) Reflected-light image of an ~9.5 cm interval spanning the uppermost Cretaceous through the lowest Paleocene in Hole 1259B; depth scale represents centimeters in core-section 13R-1. Empty spaces show up as either dark (e.g., cracks in the Danian claystone) or milky white (e.g., clouded epoxy within plucked voids near the base of the spherule layer). (B) Interpretive line drawing of features in A. Labeled boxes show approximate position of images C–F. (C) X-ray map of Fe concentrations illustrating presence of disseminated pyrite and marcasite in the upper 5 mm of the spherule bed, as well as sulfides within spherules in the middle portion of the spherule bed and as discrete grains in the Danian. (D) X-ray map of the concentration of Zn, which is present in sphalerite within a narrow portion of the spherule bed. (E) Backscattered electron micrograph of sphalerite crystals cutting across a spherule edge. (F) Plane-light photomicrograph of sulfides within the lower hemisphere of spherules from the base of the spherule bed. Widths of images C–F are ~11, 5.5, 1.2, and 4.5 mm, respectively.

Maastrichtian, the 2 cm spherule bed, and the subsequent 11 cm of the Danian. The boundary section included the 2-cm-thick spherule bed and ~2 cm each of the underlying Maastrichtian and overlying Danian sediment. Sediment textures, mineralogy, and foraminiferal distributions were described from the thin sections and confirmed with scanning electron microscope (SEM) studies and microprobe analyses.

In addition, X-ray maps of the relative abundance of major and some trace elements were generated from scans of a polished boundary section using a 5-spectrometer JEOL 8900 electron microprobe in the Department of Geology and Geophysics at the University of Minnesota. Operating conditions were: an accelerating voltage of 15 kV, beam current of 100 nA, and a dwell time of 50 ms for major elements and 80–100 ms for trace elements. Owing to the large size of the sample, X-ray mapping was conducted using a fixed beam while the stage

Figure 3. Backscattered electron micrograph of the contact between the lower white layer and the base of the spherule layer (dashed line). Small- to medium-sized, moderately preserved Cretaceous foraminifera are common in the lower white layer.

moved the sample. The spatial distribution of the elements Ca, Al, Si, K, Mg, Na, S, Sr, Fe, Cu, Co, and Zn was determined from the intensity of characteristic X-rays detected by wavelength dispersive spectrometers. The brightness (intensity) of the colors in the false-color X-ray maps qualitatively corresponds to the number of X-ray counts received for each spot (pixel) (Read, 2005).

RESULTS

Stratigraphy and Sedimentology

The K-T boundary interval at Site 1259 can be divided into three distinct lithostratigraphic intervals, the middle of which is the spherule layer. This layer separates Cretaceous chalk from Paleocene claystone that grades upward into clayey chalk over the basal few meters of the Paleocene (Fig. 2). Maastrichtian and Paleocene cores were recovered in all 13 holes (5 sites) drilled during Leg 207. Among the different sites, the Maastrichtian ranged from 30 m to 70 m thick, and the Paleocene, from 45 m to 90 m. A total length of ~400 m of Maastrichtian and ~500 m of Paleocene core was recovered. Recovery rates were generally very good, and two or three copies of the Maastrichtian and the Danian were recovered at each of the five sites, so stratigraphic recovery was effectively 100% with multiple replicates from across Demerara Rise (Erbacher et al., 2004). In those ~900 m of core, only a single horizon containing spherules was recovered in any hole, and, in each of the six holes where it was recovered, the spherule-bearing horizon occurred precisely at the contact between the Cretaceous and the Paleocene.

The spherule layer is remarkably similar among sites. In the four holes where it is well-preserved, it ranges from 1.7 to 1.9 cm thick and is composed of normally graded, grain supported, clay spherules. No sedimentary structures suggestive of traction transport or mass flows (e.g., cross-bedding, basal or internal scours, reversals or interruptions in grading) were observed. The spherule bed is olive green at its base and grades to a yellowish-green in the middle portion and is dark (due largely to the abundance of disseminated sulfides) at the top (Figs. 2A and 2B). Spherule diameters decrease from 1 to 2 mm at the base to ~0.3 mm at the top of the bed. The matrix contains well-preserved to poorly preserved Cretaceous foraminifera and is composed of clay with similar elemental concentrations as the spherules. Disseminated pyrite, chalcopyrite, and galena are common to abundant between the spherules in the top 5 mm of the spherule bed and are present within some spherules through the lower half of the spherule bed. These minerals are rare in the middle portion of the bed. Whether between or within spherules, they are not observed to cut across spherule boundaries, and, for occurrences within spherules, they are consistently found in the lower hemisphere (Figs. 2C and 2F). Sphalerite occurs as small radiating clusters of rectangular crystals that cut across spherule edges in a narrow stratigraphic interval 7–10 mm below the top of the spherule bed (Figs. 2D and 2E).

The base of the spherule bed is in sharp, locally undulatory contact with a 1–5-mm-thick white layer that grades to tan color and has a horizontal fabric (not laminations) at its base. It contains moderately to poorly preserved foraminifera (Figs. 2A and 3) and is referred to as the lower white layer (to distinguish it from a second white zone immediately above the spherule bed). The lower white layer is present in all sites where the boundary was recovered. It is finer grained and more clay rich than the underlying chalk. Foraminifera isolated from it are commonly fragmented or missing chamber faces (i.e., they show signs of moderate dissolution). In Hole 1258B, a single layer of spherules penetrates the white layer and rests directly on the subjacent unit (Shipboard Scientific Party, 2004a). Otherwise, the lower white layer has a sharp, planar contact with the underlying tan and burrow-mottled Maastrichtian chalk. The chalk contains rare pyrite and marcasite throughout. Authigenic calcite is present within many foraminiferal chambers. Our samples are from the upper ~3.5 m of the Campanian-Maastrichtian chalk unit, which is 50 m thick at Site 1259. The chalk ranges from 30 to 70 m thick at the five Leg 207 sites, and it rests on 50–90 m of Cenomanian-Santonian laminated,

organic-rich, silty claystone, in which continuing biological activity likely created a strongly reducing diagenetic environment for K-T deposits (Erbacher et al., 2004).

The upper contact of the spherule bed is also sharp and separates the spherule bed from a dark olive claystone with a basal, ~1-mm-thick white zone (the upper white zone herein). Foraminifera are rare in the claystone, and pyrite, marcasite, and authigenic calcite are present (Fig. 4). Carbonate content gradually increases upsection from ~20% in the lowest Danian to ~50% within 3 m of the boundary at Site 1259 (Shipboard Scientific Party, 2004b). The upper white zone is texturally and compositionally similar to the overlying dark olive claystone. In Hole 1259C, there is also a reddish interval from core section 8R-2, 90 cm, to 8R-5, 30 cm. The color change both into and out of the reddish interval is gradational over ~50 cm. Similar red intervals are present above the boundary at Sites 1258 and 1260, but the distance above the boundary of these red intervals varies among sites. Biostratigraphic data are not yet sufficiently refined to determine if the red intervals are temporally correlative (and thus possibly of paleoceanographic origin) or not (and thus likely reflective of local diagenetic conditions).

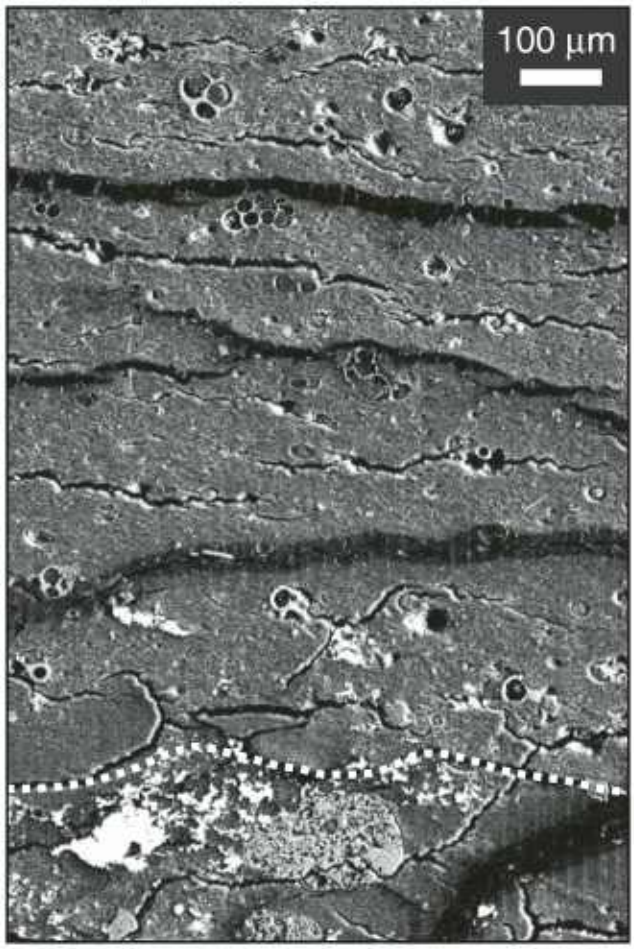

Figure 4. Backscattered electron micrograph of the basal millimeter of Danian claystone. Foraminifera in this interval are rare and are dominated by the triserial form *Guembelitria cretacea*, of which several tests are present in this image. The dashed line traces the base of the Danian claystone. The white and light-gray regions below the contact are sulfides within the uppermost spherule bed. The white regions ~100 µm above the contact are sulfides in the Danian claystone.

Foraminiferal Preservation and Biostratigraphy

Core 8R in Hole 1259C spans all or parts of 8 planktic foraminiferal zones, including both the latest Maastrichtian *Plummerita hantkeninoides* zone and the earliest Danian P0 zone (Table 1). Cretaceous foraminifera are abundant, and preservation is poor to good in the seven samples examined from below the spherule layer. Test morphology is generally well preserved, but foraminiferal chambers commonly contain crystals of sparry calcite. Foraminifera in the spherule layer and the lower white layer show considerable evidence of dissolution. In the Danian samples, foraminifera range from rare to abundant, with abundance increasing away from the spherule layer. Preservation of wall microstructure is generally good within zone P0 and lower zone Pα, moderate in upper zone Pα, and poor within subzone P1a through the top of the interval examined. Danian specimens are commonly partially or severely fragmented, and calcite infilling increases from zone Pα through the top of the studied interval. The changes in preservation correspond to changes in clay content, which would effect movement of pore fluids and, thus, diagenesis.

The lowest two samples from core 1259C-8R contain a late Maastrichtian assemblage dominated by *Rugoglobigerina* spp., *Globotruncanita* spp., and various heterohelicids. They include late Maastrichtian index fossils *Abathomphalus mayaroensis*, *Contusotruncana contusa*, *Racemiguembelina fructicosa*, and *Pseudoguembelina hariaensis*. The lowest sample examined (1259C-8R-7, 128–130 cm) contains rare specimens of the upper Campanian taxon *Radotruncana calcarata,* indicating some background reworking. Reworked *R. calcarata* were also reported from one shipboard sample from Hole 1259C (Shipboard Scientific Party, 2004b). The five highest Cretaceous samples contain a similar assemblage to the lowest two, but all also include the latest Cretaceous index species *Plummerita hantkeninoides* (Fig. 5). *P. hantkeninoides* was also observed in shipboard sample 1259C-8R-7, 66–68 cm, 12 cm above the highest sample examined in this study without this taxon (1259C-8R-7, 78–80 cm). Thus, the *P. hantkeninoides* zone is estimated at between 2.66 and 2.78 m thick, and, assuming a duration of 300,000 yr for this zone (Abramovich and Keller, 2002), the average sedimentation rate at the end of the Cretaceous was ~0.9 cm/k.y.

Cretaceous foraminifera are common in both the lower white layer and the ~2-cm-thick spherule layer. In the spherule layer, foraminifera occur in a clayey matrix between spherules and include a size range comparable to that seen in the chalk. In the lower white layer, foraminifera are smaller on average and less abundant than in the underlying chalk. In both layers, preservation of test morphology is not as good as in the chalk, and dissolution is moderate to extensive. However, foraminiferal chambers are hollow or contain fill similar to the matrix of surrounding sediment. Sparry calcite is relatively rare.

TABLE 1. THE DISTRIBUTION OF PLANKTIC FORAMINIFERA FROM 27 SAMPLES SPANNING THE CRETACEOUS-TERTIARY BOUNDARY AT SITE 1259

Sample	Depth	Age	Zone	Preservation	*Radotruncana calcarata*	*Contusotruncana contusa*	*Plummerita reicheli*	*Pseudoguembelina hariaensis*	*Pseudoguembelina palpebra*	*Rugoglobigerina rugosa*	*Globotruncanella petaloidea*	*Trinitella scotti*	*Globotruncana rosetta*	*Plummerita hantkeninoides*	*Racemiguembelina fructicosa*	*Abathomphalus mayaroensis*	*Pseudotextularia elegans*	*Hedbergella monmouthensis*	*Globotruncanita stuartiformis*	*Laeviheterohelix glabrans*	*Pseudoguembelina costulata*	*Pseudotextularia nuttalli*	*Rugoglobigerina pennyi*	*Chiloguembelina crinita*	*Chiloguembelina* sp.	*Eoglobigerina eobulloides*	*Globanomalina* cf. *fringa*	*Guembelitria cretacea*	*Hedbergella holmdelensis*	*Heterohelix globulosa*	*Parvulorugoglobigerina extensa*	*Woodringina hornerstownensis*	*Chiloguembelina midwayensis*	*Globanomalina sabina*	*Parvulorugoglobigerina eugubina*	*Parvulorugoglobigerina longiapertura*	*Chiloguembelina morsei*	*Globoconusa daubjergensis*	*Parasubbotina pseudobulloides*	*Subbotina triloculinoides*	*Globanomalina planocompressa*	*Eoglobigerina edita*	*Praemurica taurica*	*Praemurica pseudoinconstans*	*Subbotina trivialis*	*Praemurica inconstans*	*Acarinina* aff. *strabocella*	*Morozovella praeangulata*	*Praemurica uncinata*
8R-1, 18–20 cm	436.18	Danian	P3a	P																																						x	x	x	x
8R-1, 80–82 cm	436.80	Danian	P3a	M																																						x	x	x	
8R-1, 148–150 cm	437.48	Danian	P1c	P																																						x			
8R-2, 120–122 cm	438.70	Danian	P1c	P																																			x				x			
8R-3, 6–8 cm	439.06	Danian	P1c	P																																	x		x				x			
8R-3, 75–77 cm	439.75	Danian	P1b	M																				x											x		x	x						
8R-3, 128–130 cm	440.28	Danian	P1b	P																				x		x					x				x	x	x		x	x	x	x		
8R-3, 148–150 cm	440.48	Danian	P1b	P																				x		x						x					x		x	x				
8R-4, 26–28 cm	440.76	Danian	P1b	M																				x		x											x		x	x				
8R-4, 46–48 cm	440.96	Danian	P1b	P																				x		x		x				x	x				x	x						
8R-4, 60–62 cm	441.10	Danian	P1a	M																				x		x		x				x	x				x		x		x			
8R-4, 96–98 cm	441.46	Danian	P1a	M																				x		x						x	x						x				
8R-5, 0–2 cm	441.49	Danian	P1a	M																				x				x					x				x							
8R-5, 20–22 cm	441.69	Danian	P1a	M																						x					x	x		x				x		x				
8R-5, 40–42 cm	441.89	Danian	Pα	G																				x		x						x	x		x		x	x	x				
8R-5, 80–82 cm	442.29	Danian	Pα	G																						x	x	x			x	x	x		x		x	x					
8R-5, 85–87 cm	442.34	Danian	Pα	G																				x				x			x	x	x		x	x							
8R-5, 90–92 cm	442.39	Danian	P0	G						x								x						x		x	x	x			x	x	x	x	x								
8R-5, 96–98 cm	442.45	Danian	P0	G																				x	x	x	x	x	x	x	x	x											
8R-5, 99–100 cm	442.48	Danian	†	P						x					x	x	x		x	x	x	x	x																					
8R-5, 108–110 cm	442.57	Maas.	hant.	M						x		x		x	x	x																												
8R-5, 143–145 cm	442.92	Maas.	hant.	M			x		x	x				x	x	x		x																										
8R-6, 26–28 cm	443.25	Maas.	hant.	M			x		x	x		x		x																														
8R-6, 85–87 cm	443.84	Maas.	hant.	M			x			x				x		x	x																											
8R-7, 30–32 cm	444.79	Maas.	hant.	M		x	x			x			x	x	x																													
8R-7, 78–80 cm	445.27	Maas.	haria.	M		x	x	x	x	x	x	x																																
8R-7, 128–130 cm	445.77	Maas.	haria.	M	r	x	x	x	x	x																																		

Note: Depth is in meters below seafloor and represents the depth of the top of the sampled interval. Maas.—Maastrichtian; dagger—spherule layer sample; hant.—*Plummerita hantkeninoides* zone; haria.—*Psuedoguembelina harianensis* zone. Preservation is scored as good (G), moderate (M), or poor (P). For species occurrences, r for *Radotruncana calcarata* indicates suspected reworked specimens. Similar designation is not made for possibly reworked Cretaceous taxa that are present in the basal centimeters of the Paleocene.

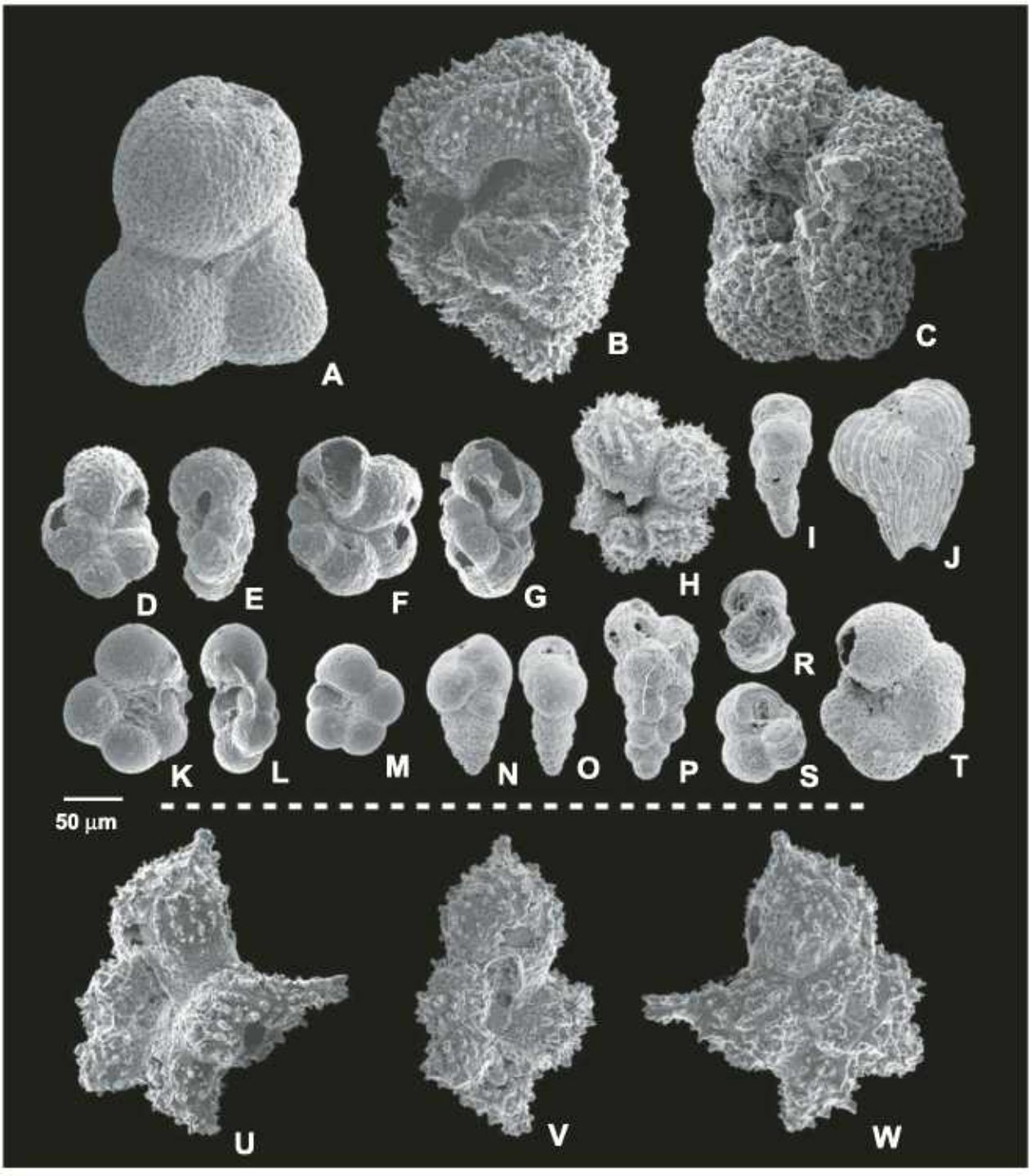

Figure 5. Selected planktic foraminifera from below and above the Cretaceous-Tertiary (K-T) boundary (separated by dashed line) at Ocean Drilling Program (ODP) Site 1259. (A) *Subbotina triloculinoides* (Plummer, 1926), sample 1259C-8R-4, 46–48 cm; (B) *Morozovella praeangulata* (Blow, 1979), sample 1259C-8R-1, 18–20 cm; (C) *Acarinina* aff. *strabocella* (Loeblich and Tappan, 1957), sample 1259C-8R-1, 18–20 cm; (D–E) *Parvularugoglobigerina eugubina* (Luterbacher and Premoli Silva, 1964), sample 1259C-8R-5, 80–82 cm; (F–G) *Parvularugoglobigerina longiapertura* (Blow, 1979), sample 1259C-8R-5, 80–82 cm; (H) *Rugoglobigerina spinosa* (Masters, 1993), sample 1259C-8R-5, 96–98 cm (probably reworked, see text); (I) *Woodringina hornerstownensis* Olsson, 1960, Sample 1259C-8R-5, 96–98 cm; (J) *Pseudoguembelina excolata* (Cushman, 1926), sample 1259C-8R-5, 96–98 cm (probably reworked, see text); (K–L) *Globanomalina* cf. *G. fringa* (Subbotina, 1953), sample 1259B- 13R-1, 46.9–46.7 cm; (M) *Globanomalina sabina* (Luterbacher and Premoli Silva, 1964), sample 1259C-8R-5, 96–98 cm; (N–O) *Chiloguembelina* sp., sample 1259C-8R-5, 96–98 cm; (P) *Guembelitria cretacea* (Cushman, 1933), sample 1259C-8R-5, 96–98 cm; (R–S) *Parvularugoglobigerina extensa* (Blow, 1979), sample 1259C-8R-5, 96–98 cm; (T) *Eoglobigerina eobulloides* (Morozova, 1959), sample 1259C-8R-5, 96–98 cm; (U–W) *Plummerita hantkeninoides* (Brönnimann, 1952), sample 1259C-8R-5, 99–100 cm.

The basal Paleocene P0 foraminiferal zone in Hole 1259C extends to 6 cm above the top of the spherule layer. The foraminiferal assemblage in sample 1259C-8R-5, 96–98 cm (an ~10 cm^3 sample of lowest Paleocene claystone and portions of the uppermost spherule layer), is dominated by small, thin-walled specimens of *Guembelitria cretacea* and benthic foraminifera. Other taxa present are rare and include small, relatively poorly preserved Cretaceous specimens, the survivor genus *Hedbergella*, and the Paleogene genera *Woodringina*, *Chiloguembelina*, and *Eoglobigerina* (Fig. 5). Examination of the boundary thin section suggests that there is a stratigraphy among foraminifera in the 2 cm interval represented by the bulk sample. Foraminiferal abundance is low immediately above the spherule layer, but *G. cretacea* dominates the assemblage within the first millimeter of the claystone (Fig. 3). Transitional forms assignable to *Woodringina* and *Chiloguembelina* are recognizable at 1 cm above the spherule layer. The first *Eoglobigerina* were recognized at ~2 cm above the spherule layer. Both size and abundance increase over this 2 cm interval for Paleogene taxa, but Cretaceous specimens are rare and small throughout. The corresponding bulk samples with 0.25 cm stratigraphic resolution from Hole 1259B confirm these size and abundance trends but show that Danian taxa do occur rarely within the first centimeter above the spherule layer.

The base of zone Pα is placed at the bottom depth for sample 1259C-8R-5, 90–92 cm, in which the lowest occurrence (LO) of *Parvularugoglobigerina eugubina* was found. The highest occurrence (HO) of *P. eugubina*, which marks the top of zone Pα, is in sample 1259C-8R-5, 40–42 cm, 58 cm above the top of the ejecta bed. *Globoconusa daubjergensis* and *Parasubbotina pseudobulloides* both have their lowest occurrences within lower zone Pα. Zone P1a extends to the LO of *Subbotina triloculinoides* in sample 1259C-8R-4, 46–48 cm, with the latter datum marking the base of subzone P1b. First appearances within subzone P1a include *Praemurica taurica* and *Eoglobigerina edita*. The base of subzone P1c is placed in sample 1259C-8R-3, 6–8 cm, which contains the LO of *Praemurica inconstans*. The presence of *Acarinina* aff. *strabocella*, *Morozovella praeangulata*, and *Praemurica uncinata* in sample 1259C-8R-1, 80–82 cm, provides the basis for identification of subzone P3a and indicates that zone P2, if present, has a maximum thickness of 66 cm (the interval between the top of sample 1259C-8R-1, 148–150 cm, and the bottom of sample 1259C-8R-1, 80–82 cm). Because demonstrable P2 samples were not found, we have not calculated sedimentation rates for subzone 1c through zone P3. However, sedimentation rates for zone P0 through subzone 1b calculated using the datums listed and ages from Berggren and Pearson (2005) range from 0.13 to 0.31 cm/k.y. for an average rate of 0.16 cm/k.y. across the first ~2 m.y. of the Cenozoic (i.e., ~20% of the rate before the boundary).

Geochemistry

X-ray maps of the relative abundances of major and trace elements illustrate well the differences among the Maastrichtian, the spherule bed, and the Danian portions of the boundary thin section (Fig. 6). The high abundance of Ca in the Maastrichtian likely reflects the high abundance of calcareous microfossils in this interval. Ca has a low abundance, and both Al and Si are abundant in the spherule layer and the overlying claystone, which is consistent with the clay-rich lithologies of these intervals. Interestingly, Mg abundance is highest in the spherule layer, whereas K is most abundant in the Danian and in clayey portions of the Maastrichtian. Sr has a similar pattern to Ca but shows less dramatic changes in concentration.

At a fine scale, Ca also shows systematic variations within each of the three intervals. Below the spherule layer, a prominent burrow in the Cretaceous chalk and the lower white layer have low-Ca and high-Si and high-Al concentrations, suggesting that these areas are more clay-rich than the surrounding sediment. Within the spherule bed, Ca is generally concentrated in the matrix surrounding spherules with a relatively high abundance in the upper half of the bed (Fig. 6). The ~2-mm-thick, Ca-rich interval at 0.7 mm above the base of the spherule bed, though, is due to a concentration of Cretaceous foraminifera of similar size to spherules at this level (Fig. 7). In the first 2 cm of Paleogene claystone, Ca concentrations are generally low but are laterally quite heterogeneous. Small, Ca-rich spots in the X-ray map correspond to individual foraminifera, whereas narrow, diffuse regions of high-Ca concentration correspond to areas with relatively more diagenetic calcite.

Sulfides are the third most common phase after carbonates and clays. S-rich zones are also enriched in Fe, Cu, and/or Zn (Fig. 6). The first two elements are more common than Zn and are closely associated with each other. Pyrite and marcasite occur as disseminated material in the uppermost 5 mm of the spherule bed (Figs. 2A and 2C) and within the lower hemisphere of spherules in the lower half of that bed (Fig. 2F). In addition, these minerals are present as well-formed sand-sized crystals throughout the pelagic and hemipelagic intervals. Zn is restricted to an ~3-mm-thick interval in the spherule bed, where it occurs in radiating clusters of rectangular sphalerite crystals that cut across spherule edges (Figs. 2D and 2E). Na abundance peaks associated with the sphalerite crystals are considered artifacts of peak overlap between Zn and Na, and neither Na nor Co exhibited obvious variations that help illuminate the K-T events at the resolution provided by our operating conditions.

The general bulk compositions of the samples do not change greatly over the 9 m studied (Table 2). Most elemental abundance ratios and normalized rare earth element (REE) abundance patterns support an upper-crustal source for detrital components throughout the sample set. However, siderophile elements show clear peaks at the top of the spherule bed, with maximum values of ~1.5 ppb for Ir, 60 ppm for Co, 100 ppm for Cr, and 200 ppm for Ni (Fig. 8). These values are significantly higher than background values above and below the boundary (Ir < 0.1 ppb, Co ~5 ppm, Ni 20–40 ppm, Cr ~30 ppm). This enrichment is equivalent to a 0.5%–1% by weight of a chondritic component. In addition, the REE patterns vary across the boundary. Above and below the spherule layer, samples exhibit similar steep C1 chondrite-normalized trends expected for terrigenous clays. REE concentrations are lower in the four Cretaceous chalk samples than in the four Danian claystone samples, which is consistent with dilution of a detrital signature by REE-poor biogenic carbonate in the Cretaceous samples. The upper spherule bed has REE contents similar to those of the Cretaceous chalk and is slightly depleted in the heavy REEs, whereas the lower spherule bed REE contents are similar to those of the Danian claystone and have a relatively high Eu concentration and slight enrichments in heavy REEs (Fig. 9). Differences in concentration within the spherule bed may reflect REEs mobilized during palagonitization of original impact glass spherules, and the patterns support a crustal origin for the majority of the spherule layer (see also Koeberl and Sigurdsson, 1992; Ortega-Huertas et al., 2002)

DISCUSSION

Evidence for Impact(s)?

The sedimentological, geochemical, and paleontological record across the K-T boundary interval at Demerara Rise is remarkably unambiguous. The spherule bed is normally graded and of very similar thickness and character among sites, suggesting a primary air-fall deposit that draped the seafloor at Demerara Rise. High concentrations of Si and Al and petrographic observations demonstrate a clay-rich lithology in the

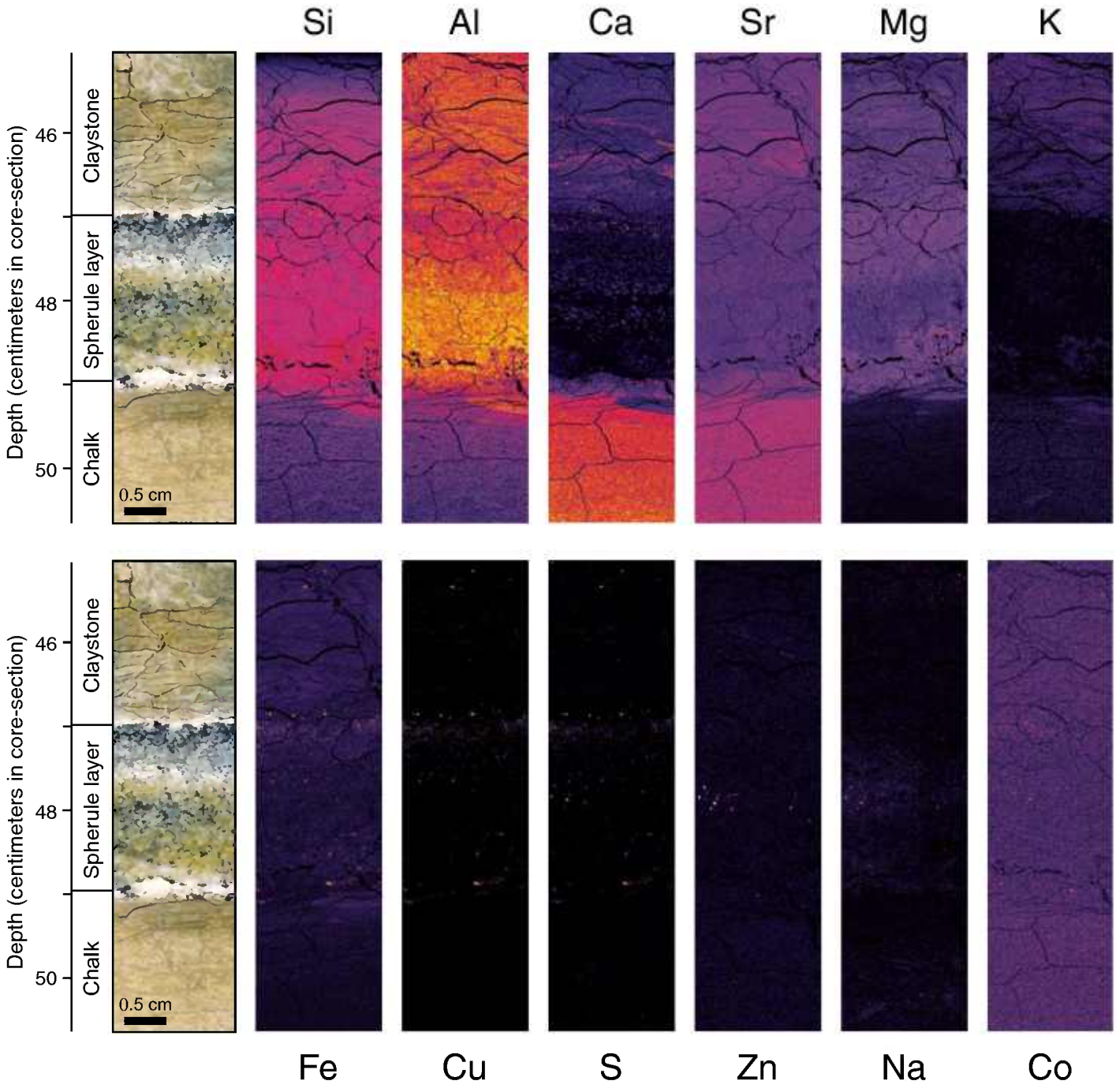

Figure 6. X-ray maps of the relative abundance of selected elements in the Cretaceous-Tertiary (K-T) boundary thin section from Ocean Drilling Program Hole 1259B. A reflected-light image of the correlative portion of the slab from which the thin section was cut is shown for reference; the depth scale represents centimeters in core-section 13R-1. The maps and reflected-light images are all at the same scale and are stratigraphically aligned, but the field of view differs slightly among maps. Cracks (dark lines in maps of Si, Al, Ca, Sr, Mg, K, Fe, and Co) and individual sulfide grains (bright spots in maps of Cu, S, Zn, and Na) allow specific position on different maps to be correlated. Colors show increasing abundance from absent (black) to peak (yellow) within the mapped area.

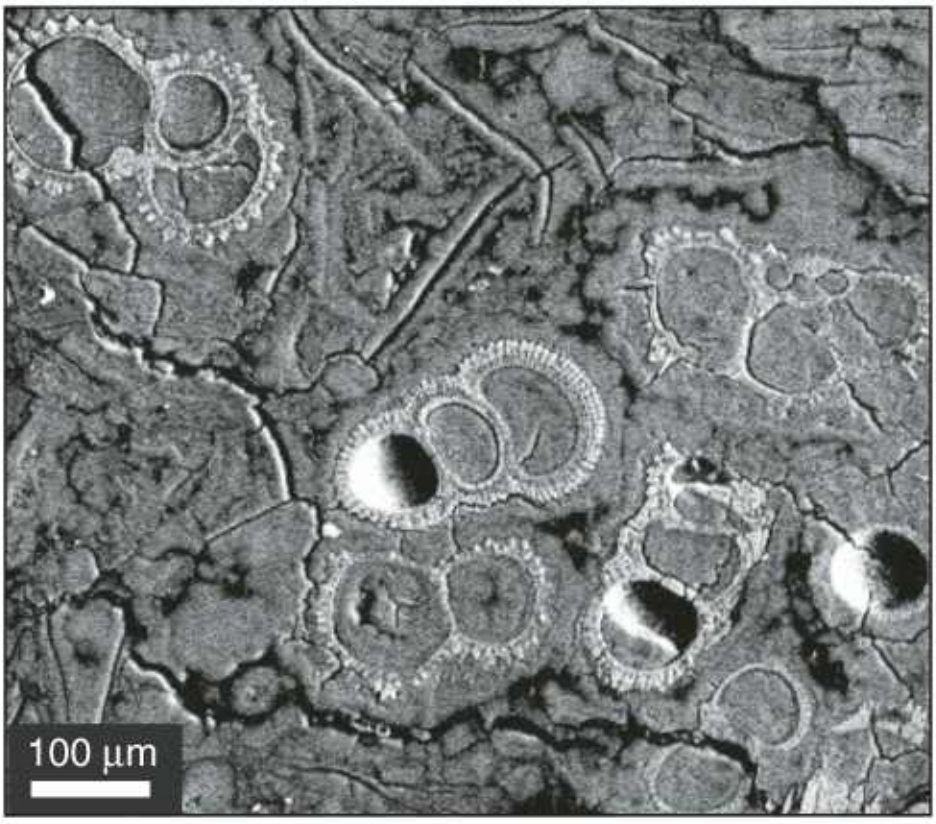

Figure 7. Backscattered electron micrograph of a concentration of Cretaceous foraminifera within the spherule layer. Chambers are either air filled (black and white) or filled with matrix from the spherule layer (medium gray), indicating that chambers were hollow when the tests were deposited. Preservation ranges from good to poor.

spherule bed, whereas the low concentrations of K and high concentrations of Mg in the layer are consistent with the spherules being impact glass altered to smectite. The distinct peak in the abundances of Ir and other siderophile elements at the top of the spherule bed supports an impact origin. Shocked minerals were not observed in the K-T thin section. However, although Demerara Rise was at an unfavorable location to receive material with the high-angle trajectory proposed for shocked basement rocks (Alvarez et al., 1995), we predict some shocked grains would be found if a large volume of the spherule bed were washed and examined.

The strongest argument against the spherule bed being the result of turbidity currents or other mass-flow processes is the uniformity of the layer across Demerara Rise. The three sites at which it was recovered are separated by ~30 km horizontally and ~0.75 km of depth, but the layer varies in thickness by only 2 mm across these distances. The lower white layer and upper white zone are present at each site, and spherule size (including grading) and the type and distribution accessory minerals (i.e., sulfides) are similar among sites. In addition, negative data supporting a primary air-fall deposit are the lack of cross-bedding, scours, or other indicators of transport processes other than settling through a water column.

Stratigraphically, the spherule bed occurs precisely at the boundary between Cretaceous and Paleocene deposits. Both the uppermost Maastrichtian *P. hantkeninoides* and lowermost Danian P0 foraminiferal zones are demonstrably present at Site 1259, and the foraminiferal assemblage underwent almost complete turnover at the boundary. Cretaceous taxa found in the basal Paleocene are small, are relatively poorly preserved, and are specimens of the most abundant small taxa in the upper Cretaceous—all of which are characteristics suggestive of reworking (e.g., Pospichal, 1996; Huber et al., 2002). Even if these specimens were survivors, though, they are a minor component of the basal Paleocene assemblage, and they do not contribute to the subsequent radiation (Olsson et al., 1999). Beyond taxonomic turnover among planktic foraminifera, the biological severity of the event is demonstrated by the dramatically lower Ca abundance (a proxy for the abundance of foraminifera and nannofossils) in the lowermost Paleocene compared to its abundance in the uppermost Cretaceous (Fig. 6).

With regard to the continuing K-T boundary controversy, the Demerara sections are as important for what they lack as for what they contain. Cumulative recovery of the Maastrichtian-Danian among the Demerara sections was excellent, and the boundary interval is biostratigraphically complete, yet the spherule bed occurs uniquely at the contact between uppermost Maastrichtian and lowermost Danian deposits. There is no sedimentological or geochemical evidence for additional impacts near the base of the *P. hantkeninoides* zone or in the lower portions of the Paleocene as proposed in multiple-impact scenarios (e.g., Keller et al., 2003). Further, qualitatively, foraminiferal assemblages do not change significantly through the 3.5 m below the boundary and show a consistent pattern of diversification across 6 m above the boundary. That is, we found no evidence for any progressive or stepwise ecological stresses before or after the extinction event at the boundary. Sedimentation rates are lower for the lower Danian than for the upper Maastrichtian, and foraminifera immediately above the boundary are better preserved on average than those below. Thus, the dramatic difference in foraminiferal abundance between the latest Maastrichtian and earliest Danian assemblages cannot be attributed to dilution or nonpreservation. In short, the Demerara sections strongly support the impact hypothesis with the primary deposits of a single impact correlated precisely with the stratigraphic level of a single, catastrophic, K-T extinction event.

The First Hours of the Paleogene

In addition to first-order agreement with predictions of the impact hypothesis, the Demerara K-T sections record and resolve the local sequence of events in fine detail, starting within minutes of the impact. Prior to impact, typical Maastrichtian pelagic deposition was occurring on an oxygenated bottom as indicated by abundant planktic foraminifera, pervasive burrow mottling, and moderate clay content in the tan Maastrichtian chalk. This facies comprises the upper Maastrichtian at Site 1259. Similar late Maastrichtian deposits are present at the other sites drilled on Demerara Rise (Erbacher et al., 2004). The prominent clay-rich burrow immediately below the lower white layer (Fig. 6) could have been active at the time of, or shortly before, the impact. If so, it may be more distinct than the background mottling because impact processes disrupted sedimentation and prevented this burrow from being overprinted by subsequent generations of burrows as the biologically mixed

TABLE 2. CONCENTRATION OF MAJOR AND TRACE ELEMENTS (PPM EXCEPT AS NOTED) FROM 23 SAMPLES SPANNING THE CRETACEOUS-TERTIARY (K-T) BOUNDARY IN CORE 1259C-8R-5

Sample	Depth	Na (wt%)	K (wt%)	Sc	Cr	Fe (wt%)	Co	Ni	Zn	As	Se	Br	Rb	Sr	Zr	Sb	Cs	Ba
8R-1, 80–82 cm	436.80	0.76	0.55	5.81	31.3	1.47	5.79	28	48	0.47	0.58	14	27.5	752	37	0.08	1.62	405
8R-2, 38–40 cm	437.88	0.45	0.44	3.54	18.1	0.66	2.54	21	39	0.77	<0.4	15	13.1	676	22	0.16	0.96	294
8R-3, 41–43 cm	439.41	0.78	<5	9.71	38.1	2.06	5.72	64	77	1.13	<0.4	15	32.7	732	123	0.31	2.14	987
8R-3, 128–130 cm	440.28	0.95	2.22	8.10	33.3	2.43	6.24	53	69	1.18	<0.5	20	44.0	789	84	0.47	2.74	732
8R-4, 1–3 cm	440.51	0.92	1.2	7.65	29.3	1.69	4.79	33	79	0.30	<0.6	19	35.9	721	83	0.19	2.29	448
8R-4, 46–48 cm	440.96	1.04	0.53	9.95	45.3	2.95	8.39	41	110	1.29	<0.9	19	48.1	679	81	0.36	3.18	525
8R-4, 96–98 cm	441.46	0.98	<3	10.60	48.5	3.18	9.21	52	98	1.20	<0.8	18	54.1	595	95	0.37	3.34	542
8R-5, 0–2 cm	441.49	1.24	<2	12.00	80.3	4.81	12.30	82	148	1.60	<0.8	20	70.3	628	123	0.58	4.34	619
8R-5, 20–22 cm	441.69	1.14	<13.2	10.70	62.9	3.44	10.50	75	106	0.90	<1.1	21	56.1	723	116	0.44	3.58	678
8R-5, 40–42 cm	441.89	1.22	<3.81	9.84	75.5	2.78	9.91	68	105	0.80	0.55	26	55.6	815	90	0.33	3.36	597
8R-5, 60–62 cm	442.09	1.09	0.57	10.80	65.2	3.03	11.40	69	106	0.60	<0.9	23	52.6	766	117	0.23	3.56	874
8R-5, 70–72 cm	442.19	1.10	<1.32	10.60	63.8	3.31	12.50	74	104	0.56	<0.9	22	57.8	760	98	0.25	3.78	548
8R-5, 80–82 cm	442.29	1.04	<7.71	10.90	67.8	2.68	12.30	82	115	1.38	<0.9	21	63.1	705	96	0.27	3.99	672
8R-5, 85–87 cm	442.34	1.03	1.17	10.50	65.1	2.48	17.40	76	107	0.56	<1.1	19	56.7	661	90	0.20	3.48	737
8R-5, 90–92 cm	442.39	1.14	1.29	11.40	73.3	3.15	39.40	134	119	4.56	<0.9	18	60.3	598	83	0.25	4.04	896
8R-5, 94–96 cm	442.43	1.32	1.22	12.70	84.6	3.62	34.40	140	204	9.85	<0.7	24	66.1	658	108	0.32	4.47	863
8R-5, 96–98 cm	442.45	1.21	1.28	11.80	78.0	3.33	34.70	153	162	11.40	0.95	22	63.7	620	98	0.45	3.86	925
8R-5, 98–99 cm	**442.47**	**1.56**	**0.45**	**15.10**	**104.0**	**2.86**	**58.50**	**195**	**545**	**41.70**	**4.93**	**20**	**21.6**	**546**	**66**	**6.27**	**1.27**	**306**
8R-5, 99–100 cm	**442.48**	**0.83**	**<5**	**9.14**	**44.0**	**1.72**	**17.50**	**97**	**414**	**13.00**	**0.14**	**15**	**35.2**	**933**	**102**	**1.98**	**1.92**	**504**
8R-5, 108–110 cm	442.57	0.51	<6.93	4.06	21.1	0.88	7.33	27	53	4.33	0.19	13	19.6	858	54	0.15	1.19	380
8R-5, 143–145 cm	442.92	0.51	<5	3.50	21.6	0.93	5.24	24	34	<1.9	<0.5	13	19.6	819	26	0.03	1.14	380
8R-7, 30–32 cm	444.79	0.64	<5	5.54	28.7	1.25	4.79	31	55	<2	<0.7	16	21.6	646	37	0.16	1.43	332
8R-7, 128–130 cm	445.77	0.79	0.74	5.92	31.0	1.56	6.22	25	51	0.50	<0.4	15	32.6	812	54	0.13	1.76	300

Note: Depth is in meters below seafloor and represents the depth of the top of the sampled interval. Samples in bold are the two samples from the spherule layer. ppm—parts per million.

(*continued*)

TABLE 2. (*continued*)

Sample	Depth	La	Ce	Nd	Sm	Eu	Gd	Tb	Tm	Yb	Lu	Hf	Ta	W	Ir (ppb)	Au (ppb)	Th	U
8R-1, 80–82 cm	436.80	14.5	26.1	12.1	2.22	0.53	2.13	0.34	0.16	1.00	0.15	0.92	0.34	0.6	<0.098	0.3	4.28	0.47
8R-2, 38–40 cm	437.88	12.3	17.9	10.2	1.75	0.38	1.45	0.26	0.14	0.90	0.14	0.52	0.21	0.7	<0.073	<0.5	3.11	0.98
8R-3, 41–43 cm	439.41	45.6	50.1	40.2	8.00	1.86	7.35	1.19	0.52	3.60	0.49	1.43	0.42	3.6	<0.16	<0.4	10.30	0.61
8R-3, 128–130 cm	440.28	24.7	42.5	20.1	3.74	0.81	3.25	0.53	0.24	1.72	0.25	1.53	0.51	2.6	<0.14	0.5	8.16	0.87
8R-4, 1–3 cm	440.51	22.3	40.9	16.4	3.56	0.76	2.76	0.46	0.25	1.68	0.22	1.32	0.46	1.2	<0.11	<0.9	7.08	0.56
8R-4, 46–48 cm	440.96	25.3	48.3	21.6	3.59	0.77	2.72	0.45	0.22	1.60	0.24	1.85	0.69	1.7	<0.25	<0.9	9.33	0.81
8R-4, 96–98 cm	441.46	29.8	51.8	22.7	4.60	0.92	3.91	0.60	0.33	2.18	0.30	2.11	0.68	<6.2	<0.31	1.0	9.14	0.78
8R-5, 0–2 cm	441.49	34.3	59.9	27.5	5.18	1.08	3.65	0.66	0.30	1.99	0.28	2.82	0.80	<4.6	<0.28	0.7	12.50	1.20
8R-5, 20–22 cm	441.69	26.6	46.1	21.2	3.83	0.81	3.37	0.51	0.24	1.70	0.25	2.26	0.77	3.8	<0.20	0.4	10.10	1.10
8R-5, 40–42 cm	441.89	23.4	37.6	16.4	3.12	0.63	2.69	0.35	0.34	1.49	0.21	2.29	0.77	<6.1	<0.19	0.6	10.20	1.41
8R-5, 60–62 cm	442.09	26.4	54.7	25.3	4.16	0.93	3.55	0.62	0.30	1.90	0.26	2.08	0.70	1.9	<0.16	1.0	9.44	0.77
8R-5, 70–72 cm	442.19	25.6	48.2	20.9	3.74	0.79	2.78	0.50	0.24	1.65	0.26	2.06	0.69	1.2	<0.18	<0.8	9.34	1.04
8R-5, 80–82 cm	442.29	29.5	56.9	24.4	4.87	1.02	4.21	0.65	0.28	2.01	0.29	2.02	0.82	<8.5	0.30 ± 0.03	0.4	9.56	1.31
8R-5, 85–87 cm	442.34	27.3	54.9	25.1	4.30	0.96	4.02	0.55	0.23	1.83	0.26	1.92	0.65	0.6	0.568 ± 0.047	0.5	8.79	1.21
8R-5, 90–92 cm	442.39	25.8	49.2	22.1	4.06	0.87	3.06	0.50	0.22	1.61	0.24	2.24	0.71	1.5	0.515 ± 0.051	0.5	9.73	1.28
8R-5, 94–96 cm	442.43	27.9	50.2	22.1	4.26	0.90	3.65	0.54	0.24	1.64	0.26	2.47	0.88	1.6	0.714 ± 0.059	1.0	11.20	1.63
8R-5, 96–98 cm	442.45	23.3	43.5	22.5	4.17	0.79	3.56	0.53	0.26	1.59	0.23	2.48	0.83	1.2	0.529 ± 0.045	<1.1	10.50	1.53
8R-5, 98–99 cm	**442.47**	**11.6**	**23.8**	**12.1**	**2.54**	**0.51**	**1.65**	**0.27**	**0.11**	**0.70**	**0.09**	**2.76**	**0.68**	**2.1**	**1.52 ± 0.07**	**0.8**	**8.12**	**3.10**
8R-5, 99–100 cm	**442.48**	**26.7**	**53.7**	**25.1**	**5.42**	**1.13**	**4.73**	**0.71**	**0.31**	**2.04**	**0.30**	**1.54**	**0.41**	**<7.2**	**0.881 ± 0.060**	**0.1**	**7.27**	**4.39**
8R-5, 108–110 cm	442.57	14.7	24.9	12.2	2.28	0.47	1.87	0.30	0.17	1.14	0.16	0.68	0.23	<6.9	0.102 ± 0.020	<0.8	2.96	2.77
8R-5, 143–145 cm	442.92	10.4	18.0	9.0	1.50	0.32	1.08	0.19	0.12	0.77	0.11	0.65	0.26	<5.8	<0.15	0.8	2.94	0.51
8R-7, 30–32 cm	444.79	18.6	27.0	15.0	2.67	0.60	2.38	0.37	0.16	1.19	0.17	0.86	0.31	<6.6	<0.21	<0.7	5.07	0.65
8R-7, 128–130 cm	445.77	16.2	29.0	12.3	2.42	0.54	1.86	0.32	0.16	1.11	0.16	1.02	0.40	<1.4	<0.23	<0.9	4.89	0.52

Note: Depth is in meters below seafloor and represents the depth of the top of the sampled interval. Samples in bold are the two samples from the spherule layer. ppb—parts per billion.

zone propagated up through the accumulating sedimentary column.

We place the K-T boundary at the contact between the tan Maastrichtian chalk and the base of the lower white layer (Fig. 2). The Global Stratotype Section and Point for the K-T boundary at El Kef, Tunisia, lies at the contact between Maastrichtian marls below and a clay layer containing indicators of impact at its base above (e.g., spherules, shocked quartz, an Ir anomaly) (Cowie et al., 1989). Using lithological correlation, the boundary on Demerara Rise would be placed at the base of the spherule bed. However, implicit in the use of impact indicators to define the boundary is the fact that the impact marks the end of the Cretaceous (Arz et al., 2004). Because of travel time through outer space, the atmosphere, and/or a water column, the first ejecta at any site arrive after the impact, and the lag time generally increases away from the impact site, albeit only on the scale of hours globally. Outside the zone of proximal ejecta (about five crater radii distance), impact-induced seismic waves travel faster than ejecta and, thus, would affect many sites before the arrival of ejecta. Shaking could result in slumping (e.g., Klaus et al., 2000) or more subtle dewatering and resuspension/elutriation of fine particles from the contemporary seafloor sediments.

The latter processes explain several characteristics of the lower white layer. The layer is finer grained, and the clay content is higher than in the underlying chalk. Preferential mobilization of fine grain sizes is expected if seismic shaking led to upward-directed fluid flow and resuspension of or elutriation from seafloor sediments. Soft-sediment deformation is common in the lower white layer (Figs. 2 and 3), including instances such as at Hole 1258B (Shipboard Scientific Party, 2004a) where spherules settled through the layer, and redeposition of material from suspension would result in a layer with high water content and low strength. Deformation is limited to the white layer and basal spherule layer, suggesting that the white layer was rheologically distinct from the underlying chalk when it was loaded by deposition of the spherule bed. However, the lower white layer is laterally persistent, again attesting to the regional uniformity of boundary processes affecting Demerara Rise. Missing chamber faces on many foraminifera in this layer and its white color despite a relatively high clay content/low carbonate content (Fig. 6) suggest bleaching and dissolution perhaps due to oxygen-rich waters being entrained by the settling spherules or caustic pore water created by alteration of impact material.

In this scenario, the lower white layer would have begun forming when seismic waves reached Demerara Rise 10–15 min after the impact.

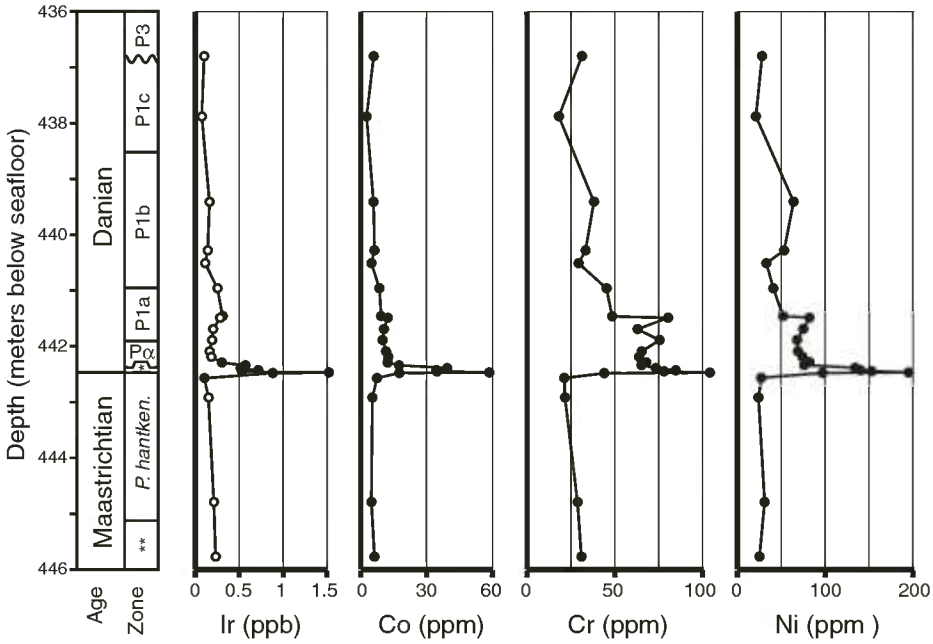

Figure 8. Concentration of Ir, Co, Cr, and Ni through core 1259C-8R-5 plotted with biostratigraphic control (Table 1) shown to the left. Under zones, symbols are as follows: ** is *Pseudoguembelina harianensis* zone, *P. hantken.* is *Plummerita hantkeninoides* zone, and * is P0 zone plus the spherule layer and lower white layer. Ir concentrations in samples plotted as hollow circles were at or below detection limits, and the value plotted represents the calculated detection limit (i.e., the maximum concentration in these samples allowed by the analyses) (Table 2). All four elements as well as other siderophiles show a dramatic peak in abundance at the top of the spherule bed. Ir concentrations return to near-background levels within ~30 cm of the spherule bed, whereas Ni concentrations remain elevated for a meter or more into the Danian.

Spherules would have arrived at the Demerara Rise sea surface about an hour after the impact (Alvarez et al., 1995). The largest spherules would have settled through a bathyal water column (~1500 m) in 1–2 h (Gibbs et al., 1971). That is, the lower white layer represents suspension and redeposition of material that occurred during the first few hours, although not the first 10 min, of the Paleocene. The smallest spherules should have settled through the water column in 10–20 d (Gibbs et al., 1971). Because there is no K-poor, Mg-rich clay interval (i.e., a lamina with elemental abundances matching the composition of the matrix in the spherule layer) above the highest spherules (Fig. 6), deposition of the matrix material in the spherule bed apparently occurred on the same weeks-to-months time scale.

Danian Foraminifera

Claystones deposited above the spherule bed exhibit a thin bleaching zone (the upper white zone) and have elemental compositions distinct from the matrix of the spherule bed, which suggests effectively continuous deposition with terrestrial clays dominant once impact material had settled. There are no apparent textural or compositional differences between the upper white zone and overlying sediments. The basal millimeters of Paleocene claystone contain a low-abundance foraminiferal assemblage dominated by *Guembelitria cretacea* and lacking *Parvularugoglobigerina eugubina* or other Paleocene taxa (that is, lower P0 zone, Fig. 5). Forms that evolved during the Paleogene first appear within 1 cm of the top of the spherule layer, and *P. eugubina* first appears 6 cm above the spherule layer. A well-resolved record of the continuing diversification of Danian foraminifera is present in the subsequent sequence, with the appearance within 2 cm above the spherule bed of *Chiloguembelina crinita*, *Parvularugoglobigerina* cf. *fringa* (= *Globigerina* cf. *fringa* of Luterbacher and Premoli Silva, 1964 and Smit, 1982), and *Woodringina hornerstownensis*. The rapid radiation of Danian planktic foraminifera continues with the appearance of additional taxa characteristic of upper zone P0, Pα, and P1a (Olsson et al., 1999). Unfortunately, authigenic calcite and dissolved or fragmented foraminifera

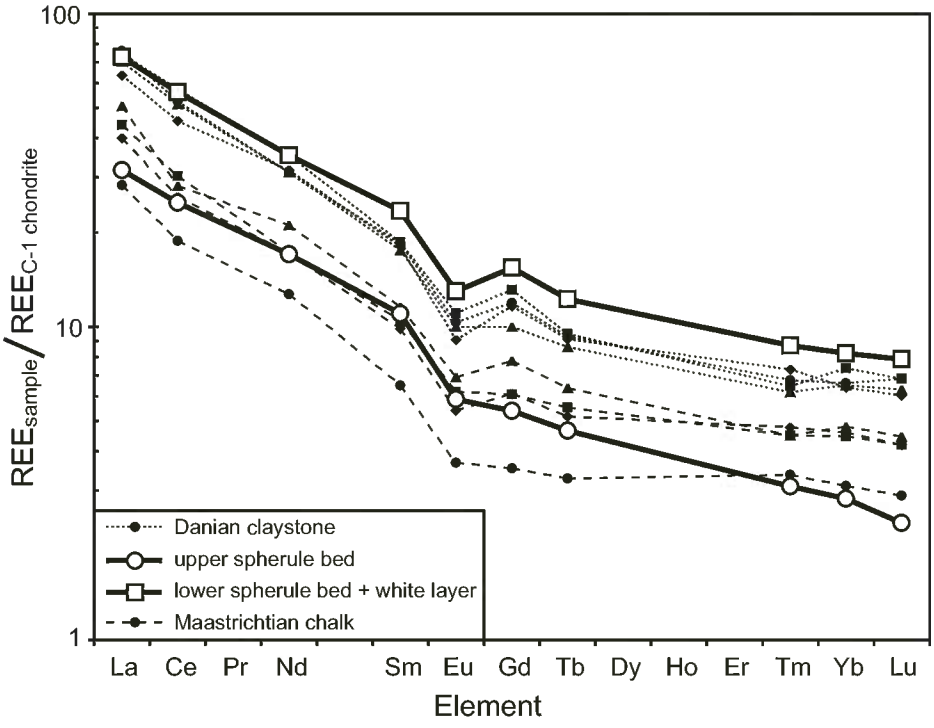

Figure 9. Rare earth element (REE) abundance (normalized to C-1 chondrites) in two samples from the spherule layer relative to patterns in the underlying and overlying units as illustrated by analyses of the four samples closest to the spherule layer. Differences in REE concentrations across the boundary likely reflect lower clay contents in the Cretaceous samples than in the Paleogene samples. Differences within the spherule bed may reflect REE mobilization during alteration of impact glasses. In all samples, the REE pattern supports a dominantly crustal origin for the REE.

are common above zone P0, which complicates any paleoceanographic or paleoecological studies of foraminiferal evolution using either stable isotopes or population counts.

During the earliest Paleocene, regional reworking was minor and local reworking was effectively absent. Although K-T reworking can be significant at distal K-T sites (e.g., Pospichal, 1996; Huber, 1996; MacLeod and Huber, 1996; Bown, 2005), the K-T stratigraphy at Demerara sites is remarkably straightforward. Cretaceous taxa are rare in the Paleocene, and there is no apparent disruption of the primary graded fabric of the spherule bed, which seems to indicate the region was not affected by a K-T tsunami. As demonstrated by the patterns of damage and distribution of casualties on 26 December 2004, a tsunami can influence regions thousands of kilometers from the source but with considerable geographic variability in effect that is not a simple function of distance from the source. Perhaps Demerara Rise was sheltered from impact-generated waves by the curve of northeastern South America. In addition, because there is no evidence of slumping (e.g., Klaus et al., 2000), local depositional slopes were presumably low enough and/or the Maastrichtian chalk was strong enough to resist large-scale failure during shaking.

Ejecta Geochemistry

The contents of Ir and other siderophile elements show peak abundances at or near the top of the ejecta layer, which suggest that material derived from the impactor was dispersed in a fine-grained phase and most reached the seafloor near the end of the accumulation of the spherule bed (e.g., Smit, 1999). Maximum values of the siderophile elements indicate up to 1% by weight of a chondritic component. Common sulfides in the top 5 mm of the spherule bed may be the remains of that fine-grained phase. Consistent with this possibility, the sulfides are found in the matrix but not in the spherules, and the stratigraphic position of the peak in Ir and other siderophile elements matches the distribution in other boundary sections (e.g., Smit, 1999). The Ir peak tails upward ~30 cm into the Danian, but Cr and Ni have elevated concentrations at least a meter into the Danian. These tails may indicate continued deposition/redeposition of exotic material long after the impact, but diagenetic mobilization (either abiotically or mediated by bacterial sulfate reduction) cannot be discounted, especially as the metals have been reduced and are present as sulfides. In fact, diagenetic alteration is the most obvious limitation of the Demerara sections. For example, the presence of sulfides only in the lower hemisphere of some spherules may reflect an original anisotropy in composition and density that led these spherules to have a preferred heavy-side-down orientation that has not subsequently been disturbed (Fig. 2F), but this pattern might also be a diagenetic fabric. Similarly, Zn is restricted to a narrow interval, but sphalerite crystals clearly cut across spherules (Fig. 2E), indicating later growth and suggesting diagenetic localization. On the other hand, the variations in Ca abundance through the spherule bed are apparently a primary fabric (Fig. 6). Cretaceous foraminifera are present throughout the spherule layer, and the presence of Ca in the matrix, especially in the upper half of the spherule bed, is interpreted to reflect the distribution of calcareous tests (whole or fragmented foraminifera and nannofossils). The Ca-rich layer ~0.7 cm above the base of the spherule bed is due to the presence of a high relative abundance of large Cretaceous foraminifera that are hollow or filled with the clayey matrix of the spherule bed (Fig. 7). These specimens have been concentrated hydrodynamically, but whether they have been locally reworked, represent regional downslope transport, or include tests that settled through the water column with the spherules (i.e., true victims of the impact) cannot be resolved with existing data.

CONCLUSIONS

At a paleodistance of ~4500 km from the Chicxulub crater, the Demerara Rise K-T sections are unusual among deep-sea sites in that they are at an intermediate distance from the crater and are unique in demonstrably including the uppermost Maastrichtian *P. hantkeninoides* and lowermost Danian P0 planktic foraminiferal zones. Foraminifera turnover (taxonomic and abundance) at the boundary is dramatic, and faunas above and below are separated by an ~2-cm-thick, graded spherule bed of impact origin. No evidence of impact is found elsewhere in the sequence. That is, the K-T record on Demerara Rise is remarkable in the degree to which it follows simple predictions given a mass extinction caused by a single impact. Sedimentological and paleontological complexities are minor, and the sections provide no support for multiple impacts or other stresses leading up to or following the

deposition of an ejecta bed. The sections also preserve fine details of the sedimentological and paleontological expression of the K-T event on Demerara Rise, including the record of resuspension of seafloor sediments within minutes of the impact, deposition of a primary air-fall layer over the subsequent hours to weeks, and a well-resolved record of the recovery and radiation of foraminifera over the first few million years of the Paleocene.

ACKNOWLEDGMENTS

We thank D. Mader for help with the neutron activation analyses, E. Goergen for microprobe assistance, P. Stanley for washing bulk samples, J. Truesdale for micrograph 2F, and M. Arthur. T. Bralower, and C. Paull for comments on an earlier draft of the manuscript. Samples were provided by the Ocean Drilling Program (ODP). ODP was sponsored by the U.S. National Science Foundation and participating countries under management of Joint Oceanographic Institutions, Inc. Funding was provided by the U.S. Science Support Program (MacLeod), the U.S. National Science Foundation (MacLeod and Huber), and the Austrian Science Foundation (Koeberl).

REFERENCES CITED

Abramovich, S., and Keller, G., 2002, High stress late Maastrichtian paleoenvironment; inference from planktonic foraminifera in Tunisia: Palaeogeography, Palaeoclimatology, Palaeoecology, v. 178, p. 145–164, doi: 10.1016/S0031-0182(01)00394-7.

Adatte, T., Keller, G., Burns, S., Stoykova, K.H., Ivanov, M.I., Vangelov, D., Kramar, U., and Stueben, D., 2002, Paleoenvironment across the Cretaceous-Tertiary transition in eastern Bulgaria, *in* Koeberl, C., and MacLeod K.G., eds., Catastrophic Events and Mass Extinctions: Impacts and Beyond: Geological Society of America Special Paper 356, p. 231–251.

Alegret, L., Arenillas, I., Arz, J.A., Diaz, C., Grajales-Nishimura, J.M., Melendez, A., Molina, E., Rojas, R., and Soria, A.R., 2005, Cretaceous-Paleogene boundary deposits at Loma Capiro, central Cuba: Evidence for the Chicxulub impact: Geology, v. 33, p. 721–724, doi: 10.1130/G21573.1.

Alvarez, L.W., Alvarez, W., Asaro, F., and Michel, H.V., 1980, Extraterrestrial cause for the Cretaceous-Tertiary extinction: Science, v. 208, p. 1095–1108.

Alvarez, W., Claeys, P., and Kieffer, S.W., 1995, Emplacement of Cretaceous-Tertiary boundary shocked quartz from Chicxulub Crater: Science, v. 269, p. 930–935.

Arz, J.A., Alegret, L., and Arenillas, I., 2004, Foraminiferal biostratigraphy and paleoenvironmental reconstruction at the Yaxcopoil-1 drill hole, Chicxulub Crater, Yucatan Peninsula: Meteoritics & Planetary Science, v. 39, p. 1099–1111.

Berggren, W.A., and Pearson, P.N., 2005, A revised tropical to subtropical Paleogene planktonic foraminiferal zonation: Journal of Foraminiferal Research, v. 35, p. 279–298, doi: 10.2113/35.4.279.

Blow, W.H., 1979, The Cainozoic Globigerinida: Leiden, E.J. Brill, 1413 p.

Bourgeois, J., Hansen, T.A., Wiberg, L., and Kauffman, E.G., 1988, A tsunami deposit at the Cretaceous-Tertiary boundary in Texas: Science, v. 241, p. 567–570.

Bown, P.R., 2005, Selective calcareous nannoplankton survivorship at the Cretaceous-Tertiary boundary: Geology, v. 33, p. 653–656, doi: 10.1130/G21566.1.

Bralower, T.J., Paull, C.K., and Leckie, R.M., 1998, The Cretaceous-Tertiary boundary cocktail: Chicxulub impact triggers margin collapse and extensive sediment gravity flows: Geology, v. 26, p. 331–334, doi: 10.1130/0091-7613(1998)026<0331:TCTBCC>2.3.CO;2.

Brönnimann, P., 1952, Globigerinidae from the Upper Cretaceous (Cenomanian-Maestrichtian) of Trinidad, B.W.I.: Bulletin of American Paleontology, v. 34, p. 1–70.

Claeys, P., Kiessling, W., and Alvarez, W., 2002, Distribution of Chicxulub ejecta at the Cretaceous-Tertiary boundary, *in* Koeberl, C., and MacLeod K.G., eds., Catastrophic Events and Mass Extinctions: Impacts and Beyond: Geological Society of America Special Paper 356, p. 55–68.

Cowie, J.W., Zieger, W., and Remane, J., 1989, Stratigraphic Commission accelerates progress, 1984–1989: Episodes, v. 112, p. 79–83.

Cushman, J.A., 1926, Some foraminifera from the Mendez shale of eastern Mexico: Contributions from the Cushman Laboratory for Foraminiferal Research, v. 2, p. 16–26.

Cushman, J.A., 1933, Some new foraminiferal genera: Contributions from the Cushman Laboratory for Foraminiferal Research, v. 9, p. 32–38.

Erbacher, J., Mosher, D.C., Malone, M.J., et al., 2004, Proceedings of the Ocean Drilling Program, Initial Reports, Volume 207: College Station, Texas, Ocean Drilling Program, Texas A&M University [CD-ROM].

Gibbs, R.J., Mathews, M.D., and Link, D.A., 1971, The relationship between sphere size and settling velocity: Journal of Sedimentary Petrology, v. 41, p. 7–18.

Ginsburg, R.N., 1997, Perspectives on the blind test: Marine Micropaleontology, v. 29, p. 101–103, doi: 10.1016/S0377-8398(96)00046-1.

Huber, B.T., 1996, Evidence for planktonic foraminifer reworking versus survivorship across the Cretaceous-Tertiary boundary at high latitudes, *in* Ryder, G., Gartner, S., and Fastovsky, D., eds., New Developments Regarding the KT Event and Other Catastrophes in Earth History: Geological Society of America Special Paper 307, p. 319–334.

Huber, B.T., MacLeod, K.G., and Norris, R.D., 2002, Abrupt extinction and subsequent reworking of Cretaceous planktonic foraminifera across the Cretaceous-Tertiary boundary: Evidence from the subtropical North Atlantic, *in* Koeberl, C., and MacLeod K.G., eds., Catastrophic Events and Mass Extinctions: Impacts and Beyond: Geological Society of America Special Paper 356, p. 277–289.

Keller, G., Li, L., Stinnesbeck, W., and Vicenzi, E., 1998, The K/T mass extinction, Chicxulub and the impact-kill effect: Bulletin de la Société Géologique de France, v. 169, p. 485–491.

Keller, G., Stinnesbeck, W., Adatte, T., and Stueben, D., 2003, Multiple impacts across the Cretaceous-Tertiary boundary: Earth-Science Reviews, v. 62, p. 327–363, doi: 10.1016/S0012-8252(02)00162-9.

Keller, G., Adatte, T., Stinnesbeck, W., Stueben, D., Berner, Z., Kramar, U., and Harting, M., 2004, More evidence that the Chicxulub impact predates the K-T mass extinction: Meteoritics & Planetary Science, v. 39, p. 1127–1144.

Klaus, A., Norris, R.D., Kroon, D., and Smit, J., 2000, Impact-induced mass wasting at the K-T boundary, Blake Nose, western North Atlantic: Geology, v. 28, p. 319–322, doi: 10.1130/0091-7613(2000)028<0319:IIMWAT>2.3.CO;2.

Koeberl, C., and Huber, H., 2000, Optimization of the multiparameter-coincidence spectrometry for the determination of iridium in geological materials: Journal of Radioanalytical and Nuclear Chemistry, v. 244, p. 655–660, doi: 10.1023/A:1006754409429.

Koeberl, C., and MacLeod, K.G., eds., 2002, Catastrophic Events and Mass Extinctions: Impacts and Beyond: Boulder, Colorado, Geological Society of America Special Paper 356, 746 p.

Koeberl, C., and Sigurdsson, H., 1992, Geochemistry of impact glasses from the K-T boundary in Haiti; relation to smectites and a new type of glass: Geochimica et Cosmochimica Acta, v. 56, p. 2113–2129, doi: 10.1016/0016-7037(92)90333-E.

Loeblich, A.R., Jr., and Tappan, H., 1957, Planktonic foraminifera of Paleocene and early Eocene age from the Gulf and Atlantic coastal plains: Washington, D.C., U.S. Government Printing Office, v. 215, p. 173–198.

Luterbacher, H.P., and Premoli Silva, I., 1964, Biostratigrafia del limite Cretaceo-Terziario nell'Appenino centrale: Rivista Italiana di Paleontologia e Stratigrafia, v. 70, p. 67–128.

MacLeod, K.G., and Huber, B.T., 1996, Strontium isotopic evidence for extensive reworking in sediments spanning the Cretaceous-Tertiary boundary at ODP Site 738: Geology, v. 24, p. 463–466, doi: 10.1130/0091-7613(1996)024<0463:SIEFER>2.3.CO;2.

MacLeod, K.G., Huber, B.T., and Fullagar, P.D., 2001, Evidence for a small (~0.000,030) but resolvable increase in seawater $^{87}Sr/^{86}Sr$ ratios across the Cretaceous-Tertiary boundary: Geology, v. 29, p. 303–306, doi: 10.1130/0091-7613(2001)029<0303:EFASBR>2.0.CO;2.

MacLeod, N., and Keller, G., 1991, Hiatus distributions and mass extinctions at the Cretaceous/Tertiary boundary: Geology, v. 19, p. 497–501, doi: 10.1130/0091-7613(1991)019<0497:HDAMEA>2.3.CO;2.

MacLeod, N., Rawson, P.F., Forey, P.L., Banner, F.T., Boudagher-Fadel, M.K., Bown, P.R., Burnett, J.A., Chambers, P., Culver, S., Evans, S.E., Jeffery, C., Kaminski, M.A., Lord, A.R., Milner, A.C., Milner, A.R., Morris, N., Owen, E., Rosen, B.R., Smith, A.B., Taylor, P.D., Urquhart, E., and Young, J.R., 1997, The Cretaceous-Tertiary biotic transition: Journal of the Geological Society of London, v. 154, Part 2, p. 265–292.

Masters, B.A., 1993, Re-evaluation of the species and subspecies of the genus *Plummerita* Brönnimann and a new species of *Rugoglobigerina* Brönnimann (Foraminiferida): Journal of Foraminiferal Research, v. 23, p. 267–274.

Morozova, V.G., 1959, Stratigrafiya Datsko-Montskikh otlozhenii Kryma po foraminiferam: Doklady Akademiya Nauk SSSR, v. 124, p. 1113–1116.

Norris, R.D., Huber, B.T., and Self-Trail, J., 1999, Synchroneity of K-T oceanic mass extinction and meteorite impact, Blake Nose, western Atlantic: Geology, v. 27, p. 419–422, doi: 10.1130/0091-7613(1999)027<0419:SOTKTO>2.3.CO;2.

Olsson, R.K., 1960. Foraminifera of Latest Cretaceous and earliest Tertiary age in the New Jersey coastal plain: Journal of Paleontology, v. 34, p. 1–58.

Olsson, R.K., Liu, C., and van Fossen, M., 1996, The Cretaceous-Tertiary catastrophic event at Miller's Ferry Alabama, *in* Ryder, G., Gartner, S., and Fastovsky, D., eds., New Developments Regarding the KT Event and Other Catastrophes in Earth History: Geological Society of America Special Paper 307, p. 263–277.

Olsson, R.K., Miller, K.G., Browning, J.V., Habib, D., and Sugarman, P.J., 1997, Ejecta layer at the Cretaceous-Tertiary boundary, Bass River, New Jersey (Ocean Drilling Program Leg 174AX): Geology, v. 25, p. 759–762, doi: 10.1130/0091-7613(1997)025<0759:ELATCT>2.3.CO;2.

Olsson, R.K., Hemleben, C., Berggren, W.A., and Huber, B.T., 1999, Atlas of Paleocene planktonic foraminifera: Smithsonian Contributions to Paleobiology: Washington, D.C., Smithsonian Institution Press, 252 p.

Ortega-Huertas, M., Martínez-Ruiz, F., Palomo, I., and Chamley, H., 2002, Review of the mineralogy of the Cretaceous-Tertiary boundary clay: Evidence supporting a major extraterrestrial catastrophic event: Clay Minerals, v. 37, p. 395–411, doi: 10.1180/0009855023730054.

Plummer, H.J., 1926, Foraminifera of the Midway Formation in Texas: Austin, University of Texas Bulletin, v. 2644, 206 p.

Pospichal, J.J., 1996, Calcareous nannoplankton mass extinction at the Cretaceous/Tertiary boundary; an update, *in* Ryder, G., Gartner, S., and Fastovsky, D., eds., New Developments Regarding the KT Event and Other Catastrophes in Earth History: Geological Society of America Special Paper 307, p. 335–360.

Read, S.J.B., 2005, Electron Microprobe Analysis and Scanning Electron Microscopy in Geology (2nd edition): Cambridge, Cambridge University Press, 206 p.

Schlanger, S.O., and Jenkyns, H.C., 1976, Cretaceous oceanic anoxic events; causes and consequences: Geologie en Mijnbouw, v. 55, p. 179–184.

Schulte, P., Speijer, R.P., Mai, H., and Kontny, A., 2006, The Cretaceous-Paleogene (K-P) boundary at Brazos, Texas: Sequence stratigraphy, depositional events and the Chicxulub impact: Sedimentary Geology, v. 184, p. 77–109, doi: 10.1016/j.sedgeo.2005.09.021.

Shipboard Scientific Party, 2004a, Site 1258, *in* Erbacher, J., Mosher, D.C., Malone, M.J., et al., Proceedings of the Ocean Drilling Program, Initial Reports, Volume 207: College Station, Texas, Ocean Drilling Program, p. 1–117 [CD-ROM].

Shipboard Scientific Party, 2004b, Site 1259, *in* Erbacher, J., Mosher, D.C., Malone, M.J., et al., Proceedings of the Ocean Drilling Program, Initial Reports, Volume 207: College Station, Texas, Ocean Drilling Program, p. 1–110 [CD-ROM].

Signor, P.W., and Lipps, J.H., 1982, Sampling bias, gradual extinction patterns and catastrophes in the fossil record, *in* Silver, L.T., and Schultz, P.H., eds., Geological Implications of Impacts of Large Asteroids and Comets on the Earth: Geological Society of America Special Paper 190, p. 353–371.

Smit, J., 1982, Extinction and evolution of planktonic foraminifera after a major impact at the Cretaceous/Tertiary boundary, *in* Silver, L.T., and Schultz, P.H., eds., Geological Implications of Impacts of Large Asteroids and Comets on Earth: Geological Society of America Special Paper 190, p. 329–352.

Smit, J., 1999, The global stratigraphy of the Cretaceous-Tertiary boundary impact ejecta: Annual Review of Earth and Planetary Sciences, v. 27, p. 75–113, doi: 10.1146/annurev.earth.27.1.75.

Smit, J., and Hertogen, J., 1980, An extraterrestrial event at the Cretaceous-Tertiary boundary: Nature, v. 285, p. 198–200, doi: 10.1038/285198a0.

Smit, J., Roep, T.B., Alvarez, W., Montanari, A., Claeys, P., Grajales-Nishimura, J.M., and Bermudez, J., 1996, Coarse-grained, clastic sandstone complex at the K-T boundary around the Gulf of Mexico: Deposition by tsunami waves induced by the Chicxulub impact?, *in* Ryder, G., Gartner, S., and Fastovsky, D., eds., New Developments Regarding the KT Event and Other Catastrophes in Earth History: Geological Society of America Special Paper 307, p. 151–182.

Smit, J., van der Gaast, S., and Lustenhouwer, W., 2004, Is the transition impact to post-impact rock complete? Some remarks based on XRF scanning, electron microprobe, and thin section analyses of the Yaxcopoil-1 core in the Chicxulub Crater: Meteoritics & Planetary Science, v. 39, p. 1113–1126.

Stinnesbeck, W., Keller, G., Schulte, P., Stueben, D., Berner, Z., Kramar, U., and Lopez-Oliva, J.G., 2002, The Cretaceous-Tertiary (K-T) boundary transition at Coxquihui, state of Veracruz, Mexico; evidence for an early Danian impact event?: Journal of South American Earth Sciences, v. 15, p. 497–509, doi: 10.1016/S0895-9811(02)00079-2.

Stüben, D., Kramar, U., Harting, M., Stinnesbeck, W., and Keller, G., 2005, High-resolution geochemical record of Cretaceous-Tertiary boundary sections in Mexico: New constraints on the K-T and Chicxulub events: Geochimica et Cosmochimica Acta, v. 69, p. 2559–2579, doi: 10.1016/j.gca.2004.11.003.

Subbotina, N.N., 1953, Fossil foraminifera of the USSR: Globigerinidae, Hantkeninidae and Globorotalidae: Trudy VNIGRI, new series 76, London and Wellingborough, Translation to English by E. Lees, Collet's Ltd., 296 p. (in Russian), 321 p. (translated).

Manuscript Received 19 December 2005
Revised Manuscript Received 29 April 2006
Manuscript Accepted 1 July 2006

Printed in the USA